Chapter 2

AOT Assisted Preparation of Polythiophene-MWCNT Core-shell Nanocomposites

2.1. Introduction

Conducting polymer-carbon nanotube nanocomposites are suitable materials for fabricating electrochemical sensors, supercapacitors, thermoelectric devices, solar cell devices, micro-electro-mechanical systems (MEMS), corrosion resistive coatings, temperature sensors, and electromagnetic interference shielding (EMI) devices.[1-12] Conducting polymer-carbon nanotube composite materials have distinctive and superior control in many properties like enhanced electrical conductivity, efficient electromagnetic wave absorbing character, sharper electrochemical responses, thermal conductivity, optical tunability, and mechanical stability.[11,13-16] The specific properties achieved by nanocomposite formation could determine its performance in device fabrication. The properties are very much dependent on the structure and constitution of nanocomposites.[11,17,18] The structure-property relationships set in the nanocomposites could also result from the order of nano dimensions involved in nanomaterials. Another advantage of using nanocomposites is that they could provide modified properties than their components.[13-21] Different conducting polymers such as polyaniline, polypyrrole, polythiophene, polyphenylenevinylene and their derivatives were reported as suitable for nanocomposite preparation.[22,23] Amongst conducting polymers, polythiophene and its derivatives are significant due to their unique electrical, thermal and optical properties. Besides that, polythiophene exhibits good environmental stability also.[22-27] Multiwalled carbon nanotubes (CNTs) are suitable materials for preparing nanocomposites with conducting polymers. Multiwalled carbon nanotubes possess a unique one-dimensional structure, large surface-to-volume ratio, stiffness, conductive nature and high mechanical strength. Carbon nanotubes find many applications in broad areas such as chemical sensors, field emission materials, hydrogen energy storage, nano-electronic devices, catalyst support and so on.[28-34]

Creating well-dispersed forms of pristine carbon nanotubes is challenging due to their high aspect ratio and self-aggregating property. Nano-dispersion of carbon nanotubes can be achieved by chemical strategies such as polymer nanocomposite formation, physical mixing with suitable stabilizing agents like block co-polymers, or surfactants as dispersants. Nanocomposite formation with suitable organic polymers is an attractive way of forming nano-dispersion, since it involves inexpensive and easy synthetic approaches.[31-40] The polymer-carbon nanotube nanocomposites formation can be accomplished viz; in-situ polymerization of monomer in the presence of dispersed

CNT or post-polymerization mixing of polymer and CNT.[15,41,42] In-situ polymerization is the appropriate method for creating nanocomposite, if the monomer is soluble in suitable solvents and the polymer formed is insoluble. The post-polymerization mixing could not be taken as an able method if the polymer has insolubility in mixing solvent. Thiophene monomer is readily soluble in almost all organic solvents; thus, in-situ polymerization can be carried out for nanocomposite preparation. Three methods of polythiophene preparation are generally reported; electropolymerization, metal-catalyzed coupling reactions and oxidative chemical polymerization.[43] Chemical oxidative polymerization is advantageous for bulk polymer production in a short reaction time and with a simple reaction setup.[44] Ferric chloride ($FeCl_3$) is the most common oxidizing agent used for the oxidative polymerization of thiophene (see **Figure 2.1. a**).[41,42,44] In-situ polymerization of thiophene in the presence of carbon nanotubes produces polythiophene-CNT nanocomposites (see **figure 2.1. b**). The sonication method can be used to create a dispersion of carbon nanotubes. Mild bath sonication helps to disperse carbon nanotubes without making many defects to the CNT's electronic structure.

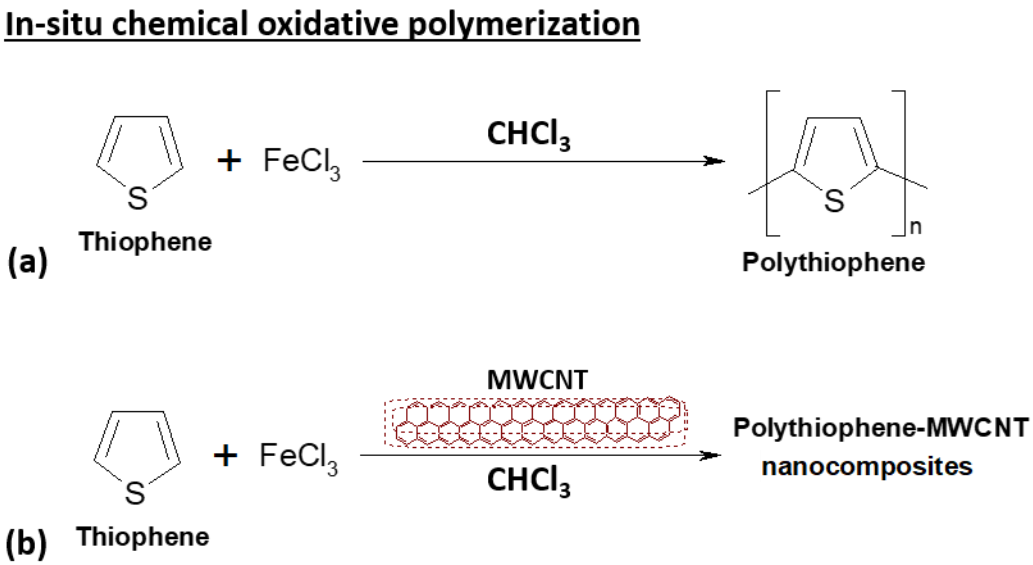

Figure 2.1. *(a) Scheme for oxidative chemical polymerization of thiophene using $FeCl_3$ oxidant and (b) in-situ chemical oxidative polymerization of polythiophene with multiwalled carbon nanotubes (MWCNT) for nanocomposite preparation.*

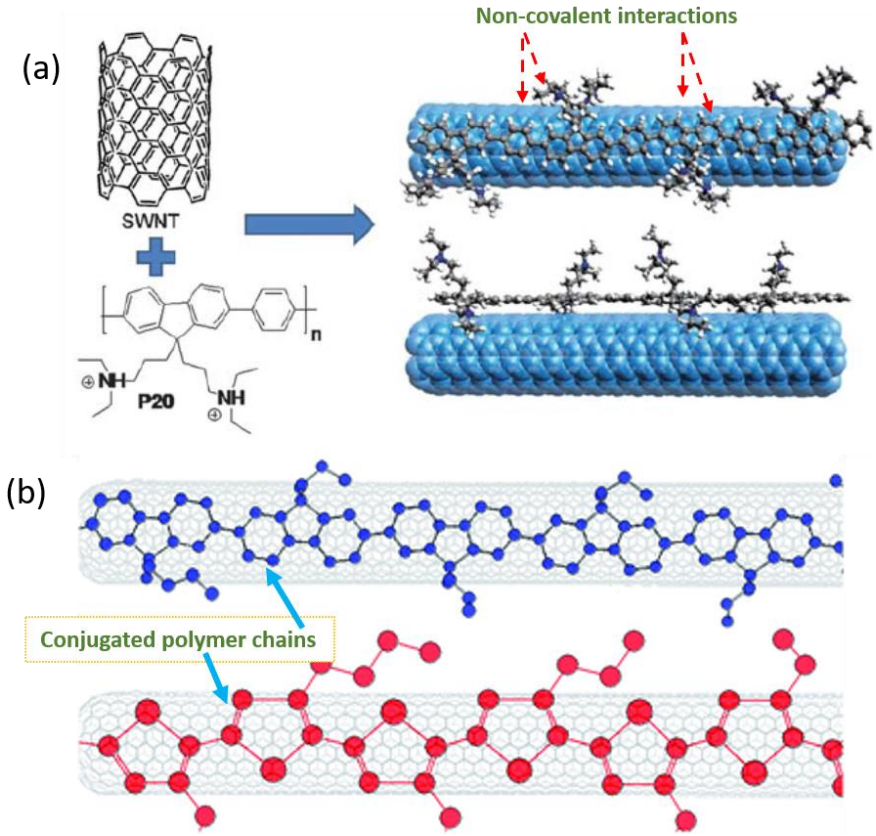

Figure 2.2. *(a) Schematic representation of interaction of carbon nanotubes with poly(9,9-bis (diethylaminopropyl)-2,7-fluoreneco-1,4-phenylene). (Adapted from Casagrande et al. 2010) and (b) illustration of the interaction of carbon nanotubes and different conducting polymers (Adapted from Tuncel 2011).*

Polybenzimidazole, polyaniline, polypyrrole, polyphenylenes, poly-phenylenevinylenes, their substituted derivatives and co-polymers could act as suitable conjugated polymer materials for nanocomposite preparation with carbon nanotubes (see **Figure 2.2.**).[35] Conjugated polymers interact with carbon nanotube surfaces via π-π stacking and van der Waals interactions leading to wrapping or adsorptive non-helical interaction. Zhai et al. functionalized carbon nanotubes with conjugated block co-polymers having non-conjugated blocks, which provided tunable functionality.[39] Lin and co-workers studied conducting polymers and reported that polymers structurally similar to CNT could act as suitable aspirants for surface functionalization.[45] Mandal et al. prepared MWCNT nanocomposite with the polymer compatibilizer containing thiophene moiety substituted with poly(dimethylamino ethyl methacrylate) (PDMAEMA) group. The authors pointed out that non-covalent functionalization on MWCNT is superior to covalent functionalization to enhance its mechanical and

electrical conductivity properties with poly(vinylidene fluoride).[46] Cho et al. designed structurally tailored multi-amphiphilic compatibilizers of pyrene-functionalized block co-polymers to attach to the walls of multiwalled carbon nanotubes (see **Figure 2.3.**). Non-covalent functionalization of CNT's surface with multi-amphiphilic compatibilizer improved dispersion stability, solubility manipulation, and hybridization with silver nanoparticles.[47]

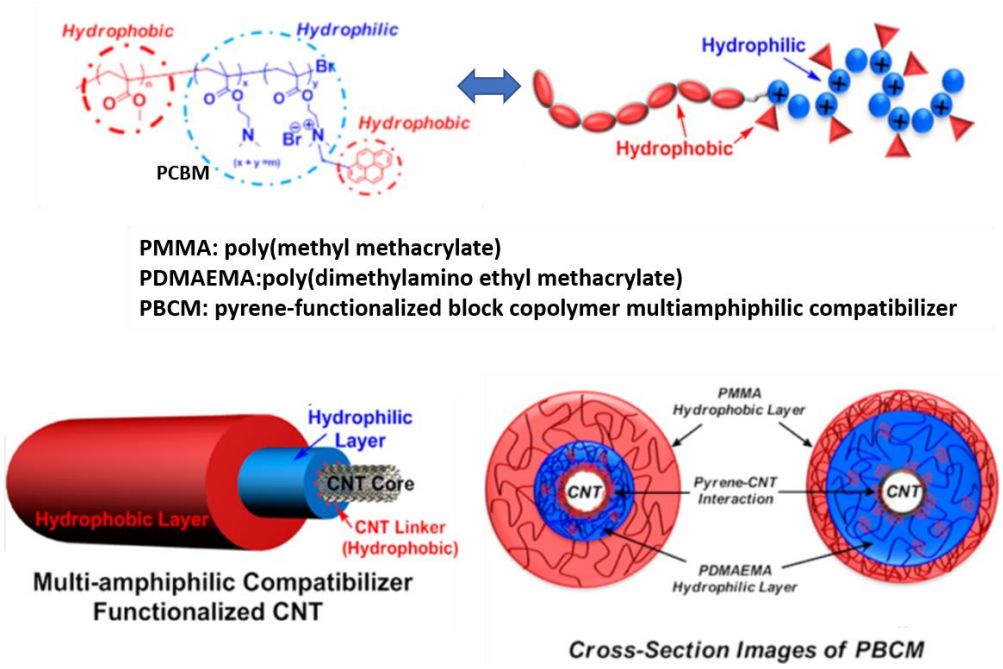

Figure 2.3. *Multiamphiphilic compatibilizer layer formations over CNT surface (adapted from Cho et al. 2015)*

Interfacial interaction between polymer and carbon nanotubes improved by adding surfactants resulting in stable dispersion and further material advancement of the system.[48] Literature studies shows different surfactants to improve the disentanglement process of CNT bundles.[48-51] Some surfactants were also reported as dopants and wetting agents for polymer-CNT structures. Surfactants have also been reported as intermediates to determine the morphological peculiarities of nanocomposites by controlling interfacial interaction between polymer and carbon nanotubes (see **Figure 2.4.**). The self-assembled nature of surfactants has the potential for constructing nanocomposites with morphology control. Surfactant assembly favourably interacts with nanocomposite constituents utilizing weak non-covalent forces like hydrogen bonding, hydrophobic effect, and van der Waals interactions. Promising polymer-surfactant complexation occurs at critical micellar concentrations

(CMC) and above; surfactant concentration should be kept at a minimum. Different types of surfactants, such as cationic, anionic, or non-ionic, exhibit distinct assembling behaviour depending on the polarity of the solvents. The intrinsic amphiphilic nature of surfactants due to polar head - non-polar tail structure facilitates two significant structural features: self-assembly formation in bulk solution and interfacial adsorption behaviour at surfaces. Micellar orientation of surfactants on the dispersed form of carbon nanotube surfaces is possible through hydrophobic interaction between the non-polar tail of surfactant molecules and hydrophobic walls of CNT (see **Figure 2.4.**).[51-53] Instead of single-tailed surfactants, the use of double-tailed surfactants can reduce interfacial tension formed due to excessive interfacial interaction in its assembled form.[54,55]

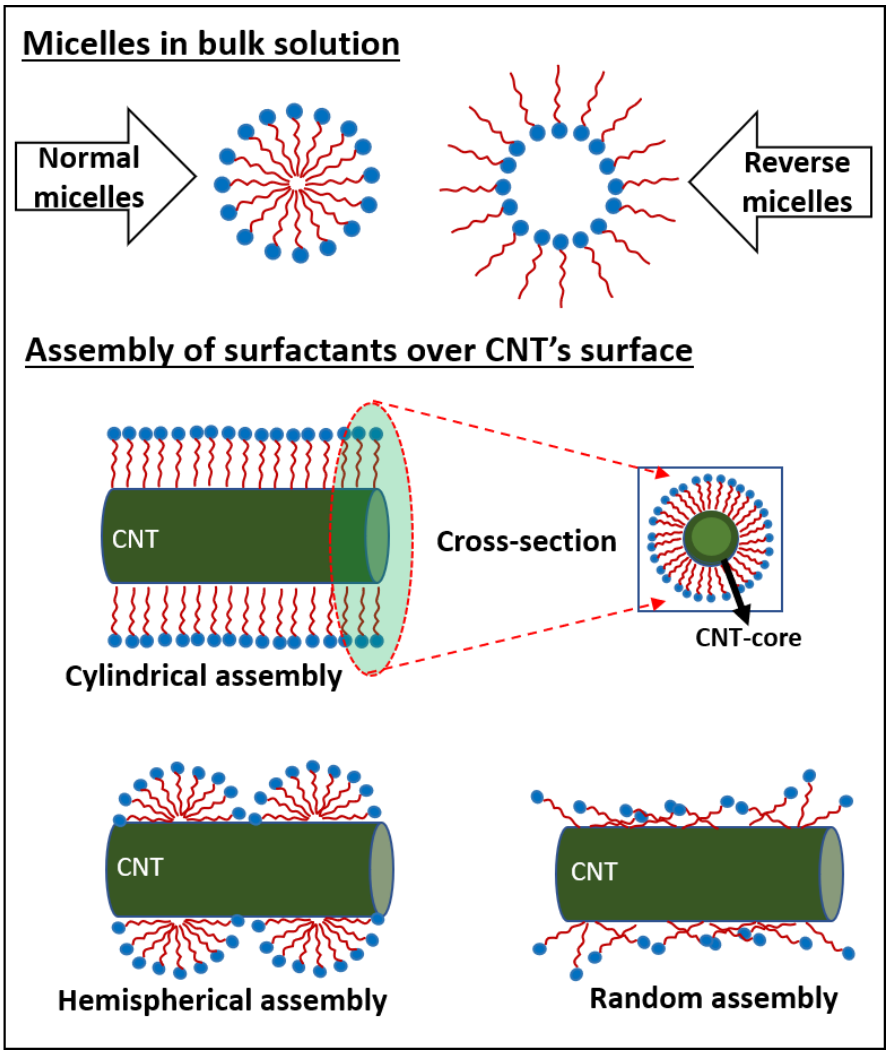

Figure 2.4. *Normal and reverse micelles formation in the bulk solution of organic solvents. Cylindrical assembly, hemispherical assembly and a random assembly of the surfactants over CNT's surface.*

In this chapter, polythiophene-multiwalled carbon nanotube nanocomposites (PTCNT) have been prepared by in-situ chemical oxidative polymerization of thiophene monomer in the presence of anionic double-tailed AOT surfactant and dispersed form of multiwalled carbon nanotubes (MWCNT) in chloroform. Oxidative polymerization was achieved with the oxidizing agent ferric chloride ($FeCl_3$). The versatile double-tailed anionic surfactant AOT [sodium bis (2-ethyl hexyl) sulfosuccinate] has its advantages, such as easy microemulsion formation without supplementing co-surfactants, double-tailed nature, good interfacial activity, and surface energy benefits in its self-assembled form.[54,55] Anionic surfactant AOT stabilizes the thiophene monomer and MWCNT via micelle interactions. MWCNT was used here as a one-dimensional tubular template for the attachment of polythiophene. Polythiophene was employed here to enhance the solubility and processability of MWCNT in a nanocomposite state. Fourier transform infrared spectroscopy (FT-IR), elemental analysis, and powder X-ray diffraction analysis (P-XRD) confirmed the nanocomposite formation. The core-shell morphology of the nanocomposite was observed by scanning electron microscopy (SEM) and high-resolution-transmission electron microscopy (HR-TEM) imaging. Stable dispersion of PTCNT nanocomposites was obtained in chloroform solvent, and UV-vis absorption spectra were recorded in their dispersed state. This chapter outlines the facile surfactant-AOT mediated in-situ polymerization strategy to develop highly ordered, conductive, dispersible, and thermally stable polythiophene-multiwalled carbon nanotube nanocomposites.

2.2. Experimental

2.2.1. Materials and reagents: Thiophene, Ferric chloride, sodium bis (2- ethyl hexyl) sulfosuccinate (AOT) and multiwalled carbon nanotubes were purchased from Sigma Aldrich. Deionized water, chloroform and acetone were purchased from Merck chemicals, India.

2.2.2. Measurements and instruments: FT-IR spectra of the samples were recorded using the KBr pellet method by Shimadzu IR Affinity 1 FT-IR spectrometer. UV-vis absorption spectra of samples were recorded using Shimadzu UV-Visible spectrometer, UV 1800 series in deionized water and HPLC-grade chloroform solvent. CHNS elemental analyses of the samples were carried out using elementar vario EL III element analyser. Powder X-ray diffraction (P-XRD) analyses of the samples were conducted

using PANALYTICAL, Aeris research with 2θ value ranging from 5°-90°. Scanning electron microscopic (SEM) imaging was conducted using JEOL Model JSM-6390LV Scanning electron microscope. High resolution transmission electron microscopic (HR-TEM) images were recorded with JEOL/JEM 2100 instrument with 200 KV with magnification 2000x-1500000x. The electrical conductivity of the samples was measured using Keithleys four probe conductivity meter. Thermogravimetric analysis (TGA) was carried out using Perkin Elmer, Diamond TG/DTA.

2.2.3. Synthesis of PTCNT-100: Monomer thiophene (1 mL, 12.50 mmol) and surfactant AOT (0.22 g, 0.50 mmol) was dissolved in chloroform (20 mL) and sonicated for 5 min. MWCNT (0.10 g) was added to the AOT-thiophene mixture in chloroform and sonicated for 10 min. The dispersed form of $FeCl_3$ in 10 mL chloroform was added drop by drop to the AOT-thiophene-MWCNT mixture and then sonicated for 15 min. Subsequently, the reaction mixture was magnetically stirred for 3 h. Polymer nanocomposite thus obtained was filtered and washed using water and acetone. The resultant composite was then dried in a vacuum oven at 60°C. Yield: 0.82 g. FT-IR (KBr, cm^{-1}) 1667, 1536, 1028 (w), 779 (w), 668. Elemental analysis (anal., wt %): C, 41.14; S, 17.80; H, 3.02.

PTCNT-200, PTCNT-300 and PTCNT-400 were prepared using the same procedure as above by changing the quantity of MWCNT as 0.20, 0.30 and 0.40 g, respectively. The figures in the sample code represent the milligrams of multiwalled carbon nanotubes used in preparing the respective nanocomposites. The samples PTCNT-200, PTCNT-300 and PTCNT-400, yielded 1.12 g, 1.16 g and 1.22 g of nanocomposite products

2.2.4. Synthesis of PTCNT-300 [AOT-0]: Monomer thiophene (1 mL, 12.50 mmol) was dissolved in chloroform (20 mL) without AOT surfactant and sonicated for 5 min. MWCNT (0.30 g) was added to the thiophene dissolved in chloroform and sonicated for 10 min. The $FeCl_3$ dispersed in 10 mL chloroform was added drop by drop to the thiophene-MWCNT mixture and then sonicated for 15 min. Subsequently, the reaction mixture was magnetically stirred for 3 h. Polymer nanocomposite thus obtained was filtered and washed using water and acetone. The resultant composite was then dried in a vacuum oven at 60°C. Yield: 0.98 g.

2.2.5. Synthesis of PT-25: Monomer thiophene (1 mL, 12.50 mmol) and surfactant AOT (0.22 g, 0.50 mmol) was dissolved in chloroform (20 mL) and sonicated for 5 min. The $FeCl_3$ dispersed in 10 mL chloroform was added drop by drop to the AOT-thiophene mixture and then sonicated for 15 min. Subsequently, the reaction mixture was magnetically stirred for 3 h. The brown powder formed was filtered and washed using water and acetone. The resultant polythiophene obtained was then dried in a vacuum oven at 60°C. Yield = 0.58 g. FT-IR (KBr, cm^{-1}) 1658, 1526, 1326, 1112, 1025, 787 and 688. Elemental analysis (anal., wt %): C, 53.73; S, 31.21; H, 3.74.

2.2.6. Synthesis of PT-25[AOT-0]: Monomer thiophene (1 mL, 12.50 mmol) was dissolved in chloroform (20 mL) without AOT surfactant and sonicated for 5 min. The dispersed form of $FeCl_3$ in 10 mL chloroform was added drop by drop to the thiophene-$CHCl_3$ mixture and then sonicated for 15 min. Subsequently, the reaction mixture was magnetically stirred for 3 h. A brown powder thus formed was filtered and washed using water and acetone. The resultant polythiophene obtained was then dried in a vacuum oven at 60°C. Yield = 0.62 g. Elemental analysis (anal., wt %): C, 44.97; S, 26.71; H, 2.89.

2.3. Results and discussion

2.3.1. Synthesis of polythiophene and polythiophene-MWCNT nanocomposites

Polythiophene-multiwalled carbon nanotube nanocomposites (PTCNTs) were prepared by in-situ chemical oxidative polymerization of thiophene in the presence of multiwalled carbon nanotubes (MWCNT) and surfactant sodium bis (2-ethyl hexyl) sulfosuccinate (AOT) in chloroform solvent (see **Figure 2.5.**). Polythiophene (PT) was polymerized using ferric chloride as an oxidant in chloroform with and without using surfactant AOT were represented as PT-25 and PT-25[AOT-0]. Surfactant AOT was added to the reaction medium to form micelles that stabilize the monomer and act as a dopant in the conducting polymer structure. In PT-25, thiophene was added to the solution of AOT in chloroform solvent; consequently, a thiophene-AOT complex micelles combination was obtained (see **Figure 2.6.**).[55-57] Polymerization of thiophene and in-situ nanocomposite formation were carried out using $FeCl_3$. The addition of AOT surfactant resulted in improved dispersion of MWCNT in chloroform by reducing the bundling forces between nanotubes.[50]

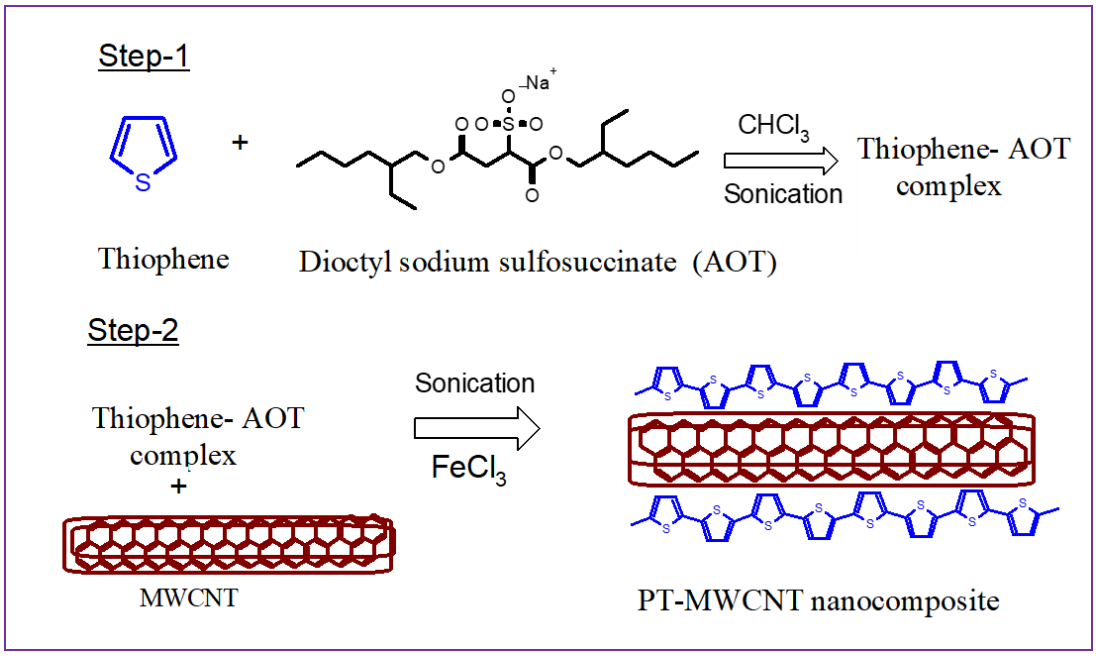

Figure 2.5. *Schematic representation of the synthesis of polythiophene-MWCNT nanocomposite (PTCNT) in presence of AOT.*

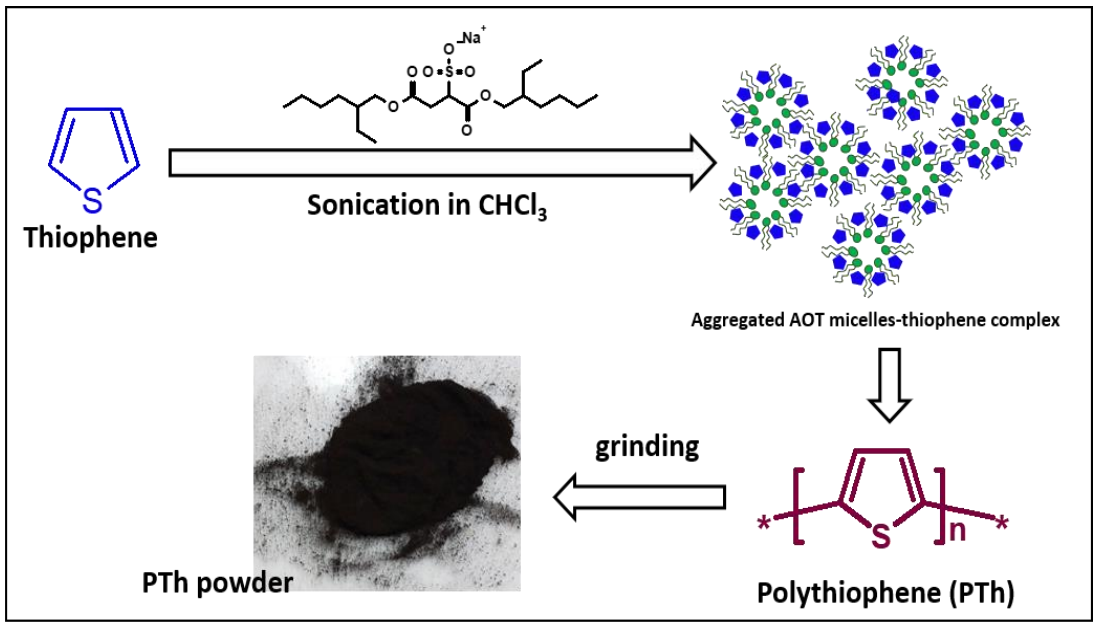

Figure 2.6. *Schematic representation of the synthesis of PT-25 in presence of AOT*

Table 2.1. *Polythiophene (PT) and PTCNT nanocomposite samples with the amount of thiophene, AOT and MWCNT, monomer to surfactant mole ratio, monomer to $FeCl_3$ mole ratio and yield obtained in the preparation.*

Sample	**Thiophene (mmol)**	**AOT (mmol)**	**MWCNT (mg)**	**Monomer/AOT mole ratio**	**Monomer/$FeCl_3$ mole ratio**	**Yield (mg)**
PT-25	12.50	0.50	0	1 :1/25	1 :1.2	584
PT-25[AOT-0]	12.50	0	0	NA	1 :1.2	620
PTCNT-100	12.50	0.50	100	1 :1/25	1 :1.2	829
PTCNT-200	12.50	0.50	200	1 :1/25	1 :1.2	1115
PTCNT-300	12.50	0.50	300	1 :1/25	1 :1.2	1166
PTCNT-400	12.50	0.50	400	1 :1/25	1 :1.2	1211
PTCNT-300[AOT-0]	12.50	0	300	NA	1 :1.2	960

In-situ chemical oxidative polymerization of thiophene was carried out in the presence of MWCNT to result in polythiophene-MWCNT nanocomposites in one step. Polythiophene (PT-25) was prepared by chemical oxidative polymerization technique using $FeCl_3$ as an oxidant in the presence of surfactant AOT in chloroform medium. Oxidative polymerization of thiophene without surfactant AOT forms polythiophene PT-25[AOT-0]. The monomer (thiophene) to surfactant (AOT) mole ratio was taken as 1:1/25, twenty-five times lower than monomer concentration and denoted as PT-25. The monomer (thiophene) to oxidant ($FeCl_3$) mole ratio was 1:1.2, a slight excess ferric chloride than monomer.[41,42,44] Chemical oxidative polymerization of thiophene in the presence of MWCNT resulted in the simultaneous production of PTCNT nanocomposites with respective compositions. The amount of MWCNT was varied as 100 mg, 200 mg, 300 mg and 400 mg (~10 to 40 weight % of thiophene monomer) to prepare four different compositions of nanocomposites such as PTCNT-100, PTCNT-200, PTCNT-300 and PTCNT-400 respectively. PTCNT-300 [AOT-0] was also prepared using the same synthetic procedure of PTCNT-300 without supplementing the AOT surfactant. The addition of ferric chloride to the AOT-thiophene mixture in chloroform resulted in a dark brown-colored polythiophene powder as the final product. More than 80% yield (polythiophene product) was obtained from the synthesis after

washing, filtration and drying. The quantity of each reagent taken for the preparation of PT-0, PT-25 and PTCNT composites and corresponding yields obtained are given in **Table 2.1.**

2.3.2. Characterization of PT and PTCNT nanocomposites

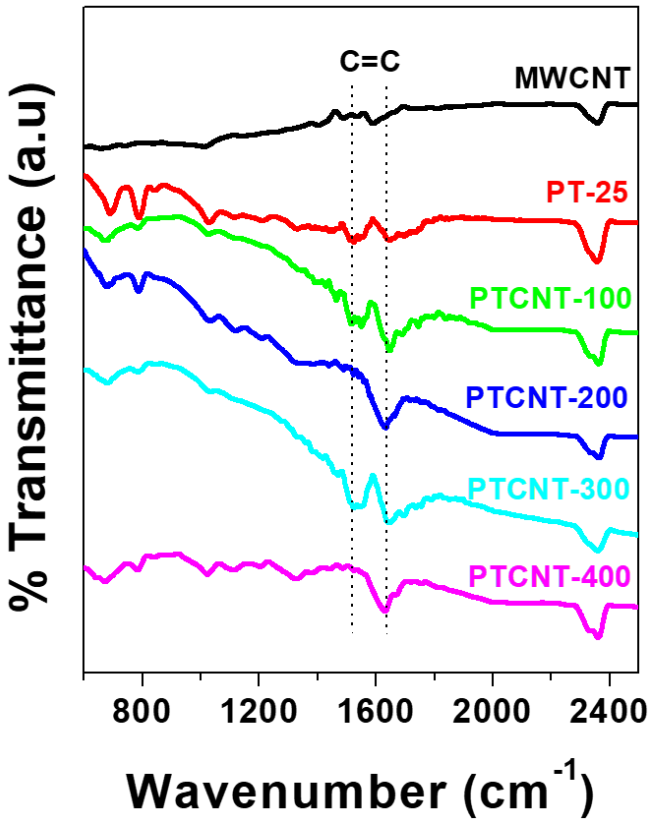

Figure 2.7. *FT-IR spectra of MWCNT, PT-25, PTCNT-100, PTCNT-200, PTCNT-300 and PTCNT-400*

Fourier transform infrared spectroscopy (FT-IR) analysis was carried out to characterize polythiophene-MWCNT nanocomposites by preparing thin pellets of samples with KBr. FT-IR spectra of PTCNT nanocomposites were compared with MWCNT and polythiophene (PT-25) (see **Figure 2.7.**). Characteristic peaks of MWCNT corresponding to aromatic asymmetric and symmetric stretching were very weak owing to the good symmetric nature of carbon nanotubes resulting in poor dipole moment changes. FT-IR spectrum of PT-25 exhibited peaks at 1658, 1526, 1326, 1112, 1025, 787 and 688 cm^{-1}. The strong peak appeared at 1658 and 1526 cm^{-1} due to C=C asymmetric and symmetric stretching contribution from thiophene ring moiety. The C-S stretching and the C-S out of plane bending deformation mode vibrations arise at 688 and 787 cm^{-1} respectively.[58-62] FT-IR spectra of PTCNT composites (PTCNT-100,

PTCNT-200, PTCNT-300 and PTCNT-400) have characteristic peaks of polythiophene. The characteristic C-S vibrations of polythiophene at 688 cm^{-1} and 787 cm^{-1} appeared weak in nanocomposites as the multiwalled carbon nanotube interaction increased in the composite. At the same time, characteristic stretching vibrations of thiophene ring moiety at 1658 and 1526 cm^{-1} in the nanocomposites were more intense than PT-25 due to the appearance of sp^2 hybridized aromatic asymmetric and symmetric stretching of carbon nanotubes in the same regions.

Table 2.2. *Elemental analysis data of sulfur, carbon and hydrogen in PT-25, PT-25[AOT-0], PTCNT-100 and PTCNT-300*

Sample	**Element present (%)**			**C/S ratio**
	Sulfur	**Carbon**	**Hydrogen**	
PT-25	31.21	53.73	3.74	1.72
PT-25[AOT-0]	26.71	44.97	2.89	1.68
PTCNT-100	17.80	41.14	3.02	2.31
PTCNT-300	18.60	56.21	1.80	3.02

*C/S ratio is ratio of percentage of carbon and sulfur obtained from elemental analysis.

Elemental analysis (CHNS analysis) was conducted for PT-25, PT-25[AOT-0], PTCNT-100 and PTCNT-300 in order to analyse the percentage of carbon, sulfur and hydrogen present in the samples (see **Table 2.2.**). Among the samples, the overall weight percentage of sulfur was highest in polymer PT-25. The higher percentage of sulfur, carbon and hydrogen in PT-25 compared to PT-25[AOT-0] was due to the incorporation of sulfur-containing AOT surfactant in the former via doping. The sulfur amount is less for composites than polymers because grouping of PT with carbon nanotubes decreases the fraction of sulfur in nanocomposite samples. The percentage of sulfur in PTCNT-300 and PTCNT-100 are relatively in the same range. The percentage of carbon was highest in PTCNT-300, as it contained the highest proportion of carbon nanotubes. The percentage of hydrogen obtained from the analysis was highest in polymeric form, whereas in carbon nanotube composites, the hydrogen content decreases. The ratio of carbon to sulphur percentage from elemental analysis in PT-25, PT-25 [AOT-0], PTCNT-100 and PTCNT-200 was calculated as 1.72, 1.68, 2.31 and 3.02 respectively. PT-25 exhibit higher carbon to sulfur ratio than PT-25 [AOT-0], due to the incorporation of AOT surfactant containing carbon bearing long

hexyl and ethyl chains. In PTCNT-100, the carbon to sulphur ratio is greater compared to PT-25. This might be due to incorporation of carbon nanotubes in PTCNT-100. The carbon to sulfr ratio is further increases in PTCNT-200 and PTCNT-300 as we add more amount of carbon nanotubes in former one (see **Table 2.2**).

Powder X-ray diffraction analysis was carried out to study the solid-state ordering of PTCNT nanocomposites formed (see **Figure 2.8. A**). Diffraction pattern of

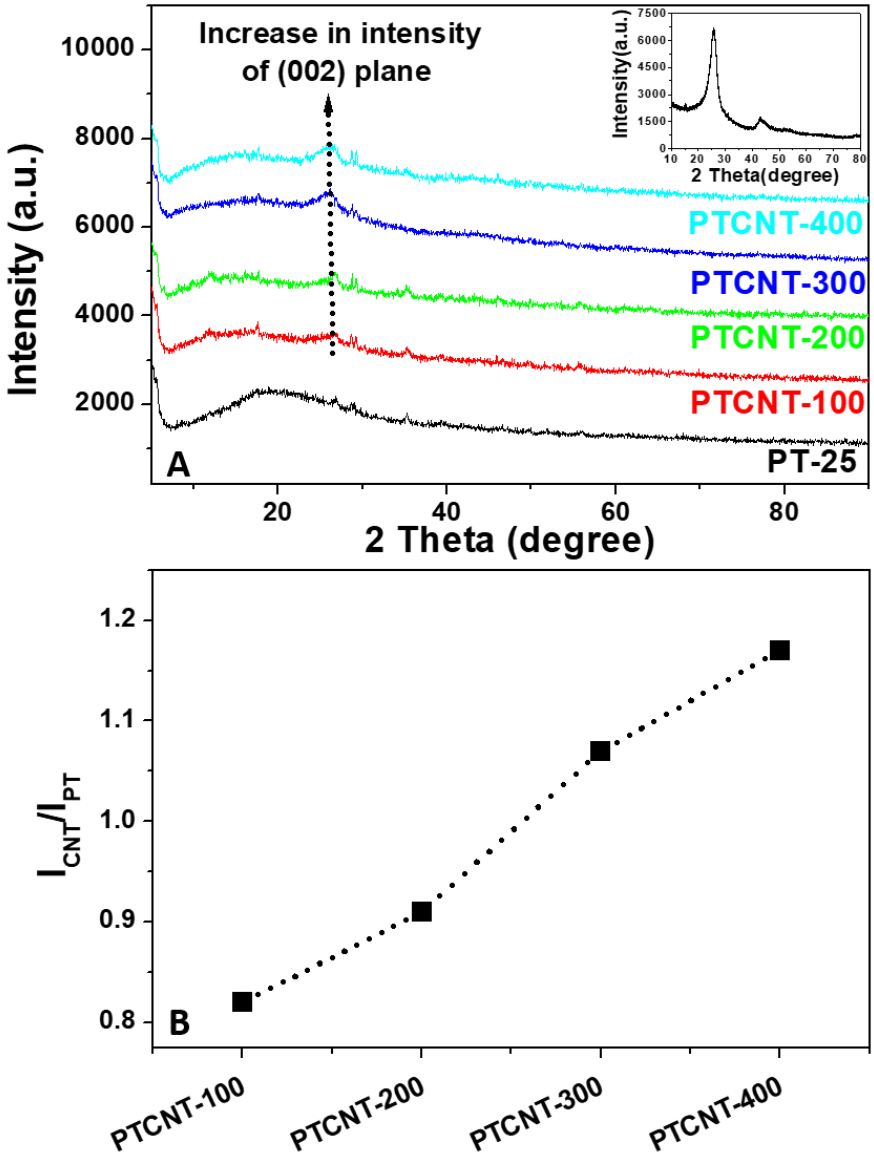

Figure 2.8. *(A) Powder X-ray diffraction patterns of PT-25, PTCNT-100, PTCNT-200, PTCNT-300 and PTCNT-400. (B) A diagram exhibiting the ratio of* I_{CNT} *(intensity of the characteristic peak of MWCNT) to* I_{PT} *(intensity of characteristic X-ray diffraction peak of polythiophene) for PTCNT composites.*

PT-25 showed an amorphous peak between 2θ values 12° and 25° with a maximum centered at 17.7°, representing the amorphous domain of polymer. MWCNT gave a diffraction pattern at 2θ value 26.10°, attributing to (002) diffraction plane between concentric layers of multiwalled carbon nanotubes.[63,64] Characteristic peaks due to (002) diffraction plane of carbon nanotubes is shown in the inset of **figure 2.8.A**. Among the nanocomposites, the intensity of the characteristic diffraction peak from (002) plane of carbon nanotubes increases for the increasing weight percentage of MWCNT, due to which the peak is more prominent in PTCNT-300 and PTCNT-400. The ratio of the intensity maximum of the characteristic peak of carbon nanotubes (I_{CNT}) to the intensity maximum of polythiophene diffraction peak (I_{PT}) was calculated for PTCNT-100, PTCNT-200, PTCNT-300 and PTCNT-400 as 0.82, 0.90, 1.07 and 1.17 respectively (see **Figure 2.8. B**). PTCNT-100 exhibited the lowest and PTCNT-400 had the highest I_{CNT}/I_{PT} value. The intensity ratio increased with the increasing weight percentage of MWCNT in the nanocomposites. The decrease of the amorphous domain of polythiophene with MWCNT nanocomposites also denotes that the amorphous domain is considerably suppressed via wrapping polymer chains around the MWCNT walls. The area corresponding to amorphous region (2θ = 12 to 25°) of PT-25 was higher than PTCNT nanocomposites (see Figure 2.9 A). The suppressed amorphous area of PTCNT nanocomposites reveals that the PTCNT composites exhibited better solid state ordering compared to PT-25. The area under crystalline peak at 2θ = 26.10° of PTCNT composites increased with the addition of MCNT to the PT-25 (Figure 2.9 B).

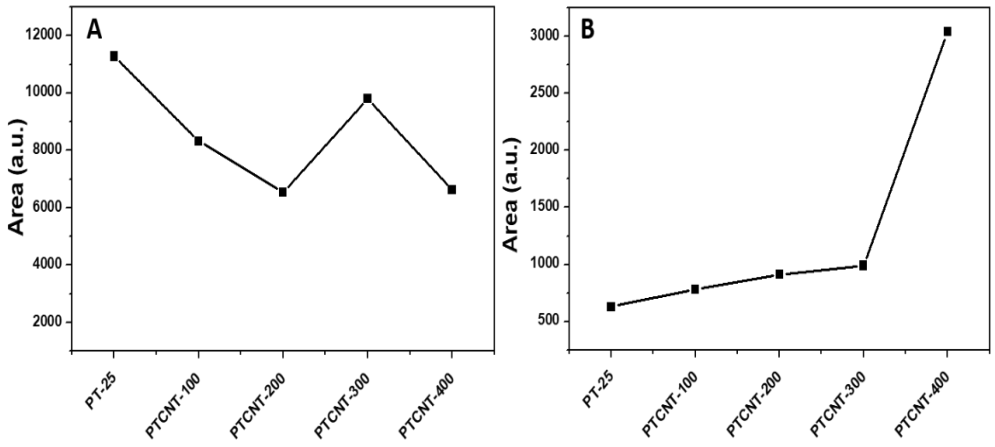

Figure 2.9. *Area under the X-ray diffraction peaks of A) amorphous region and B) crystalline region in PT-25 and PTCNT nanocomposites.*

2.3.3. Morphological characteristics of PT and PTCNT nanocomposites

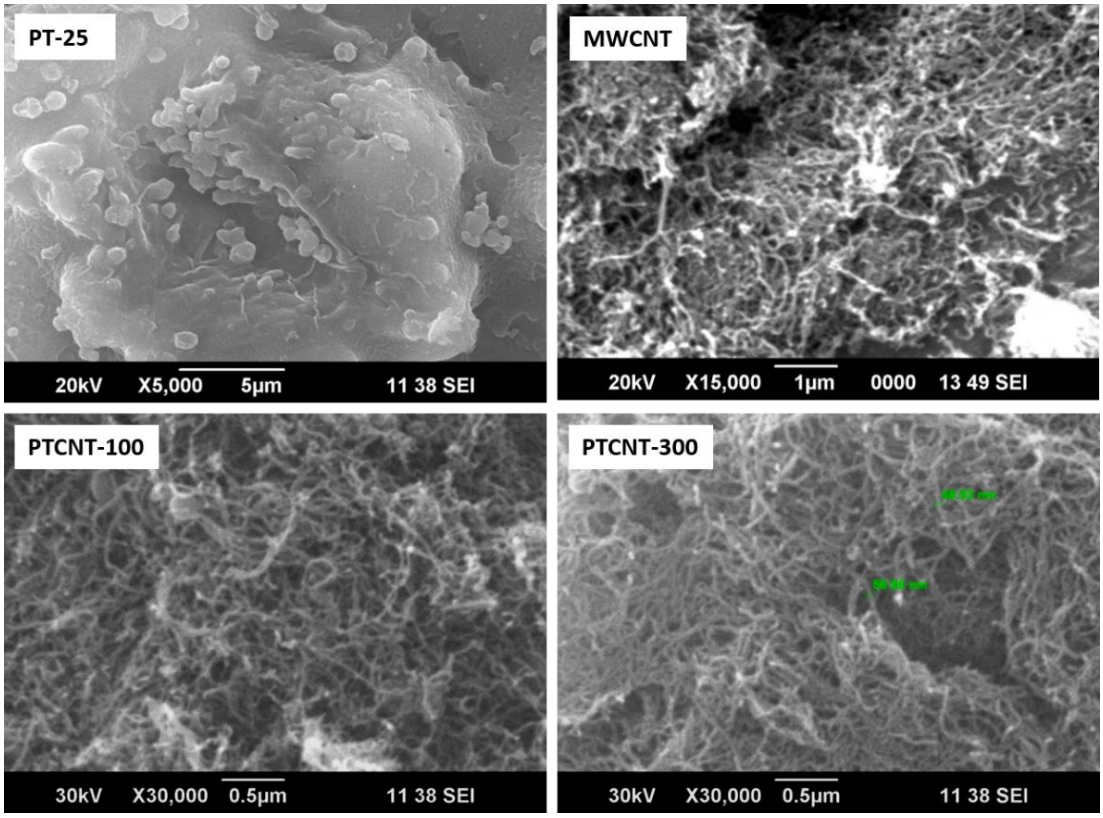

Figure 2.10. *Scanning electron microscopic (SEM) images of PT-25, MWCNT, PTCNT-100 and PTCNT-300*

Scanning electron microscopic analyses were carried out to examine the morphology of polythiophene and polythiophene-MWCNT nanocomposites (see **Figure 2.10.**). Polythiophene appeared as sub-microspherical particles, whereas PTCNTs (PTCNT-100 and PTCNT-300) exhibited fibre-like nanostructures. Nanofibrous morphology observed in PTCNT nanocomposites was matching with the inherent nanotubular structure of MWCNT. Nanocomposites attained nanofibrous morphology since growing chain of polythiophene was attached on the surface of dispersed MWCNT during polymerization. This revealed that MWCNT performed as a template in the nanocomposite formation by regulating the morphology of PTCNTs to a nanofibrous frame.

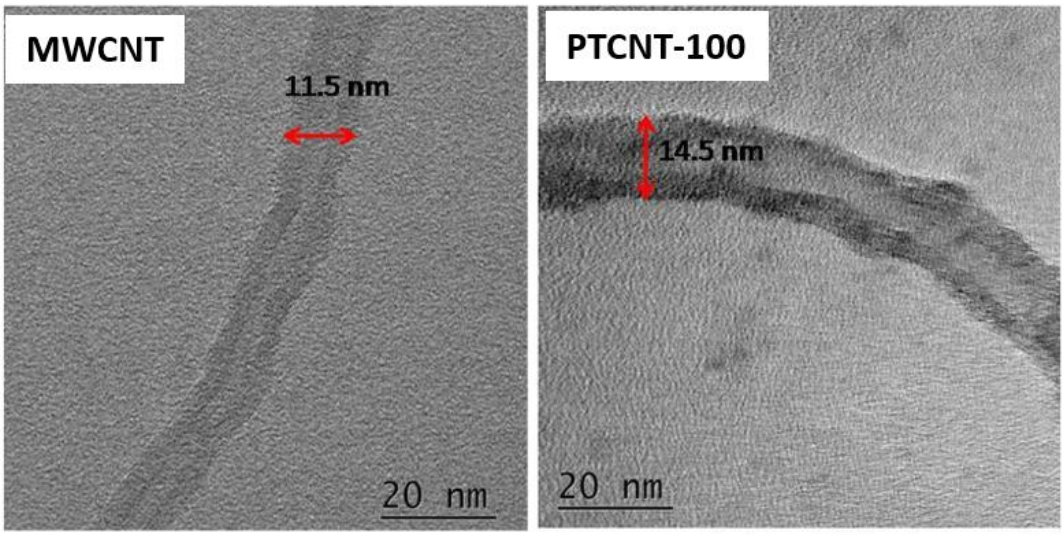

Figure 2.11. *TEM images of MWCNT and PTCNT-100 and size calculation*

Transmission electron microscopic (TEM) analysis was used to ascertain the nanocomposite size and other physical characteristics (see **Figure 2.11.** and **Figure 2.12.**). Multiwalled carbon nanotubes contained an inner unfilled lighter area, indicating the tubular structure in its TEM images. An outer layer of carbon nanotube was visible as a dark area covering the inner tube.[41,42] The average inner diameter of carbon nanotube and PTCNT-100 nanocomposites was 5 nm. The outer diameter of MWCNT was observed to be 12±2 nm, whereas the outer diameter in PTCNT-100 composites was observed to be increased from 3 to 15 nm compared to pristine CNT. The thick outer layer of PTCNT-100 composite was observed around the surface MWCNT. The result indicated that polythiophene was grown as an outer shell around the surface of carbon nanotubes. Therefore, the polythiophene-MWCNT nanocomposite could be understood as a core-shell nanotubular structure; a thick outer shell was growing up around the inner tubular MWCNT core.

2.3.4. Role of AOT in the formation of nanocomposite

The role of AOT in the formation of nanocomposites PTCNTs was ascertained using transmission electron microscopy. PTCNT-300-[AOT-0] appeared as phase-separated; on the other hand, PTCNT-100 and PTCNT-300 seemed to have the same nanofibrous morphology of MWCNT without having a separated polythiophene matrix. (see **Figure 2.12.**).[41,42] This revealed the importance of surfactant AOT for the PTCNT's nanotubular structure formation. The composite prepared without adding AOT surfactant largely retained bulk polymer mass separated from the carbon nanotube

surfaces. The AOT supports the growth of polythiophene chains around the tubular MWCNT template for effective core-shell nanocomposite formation.

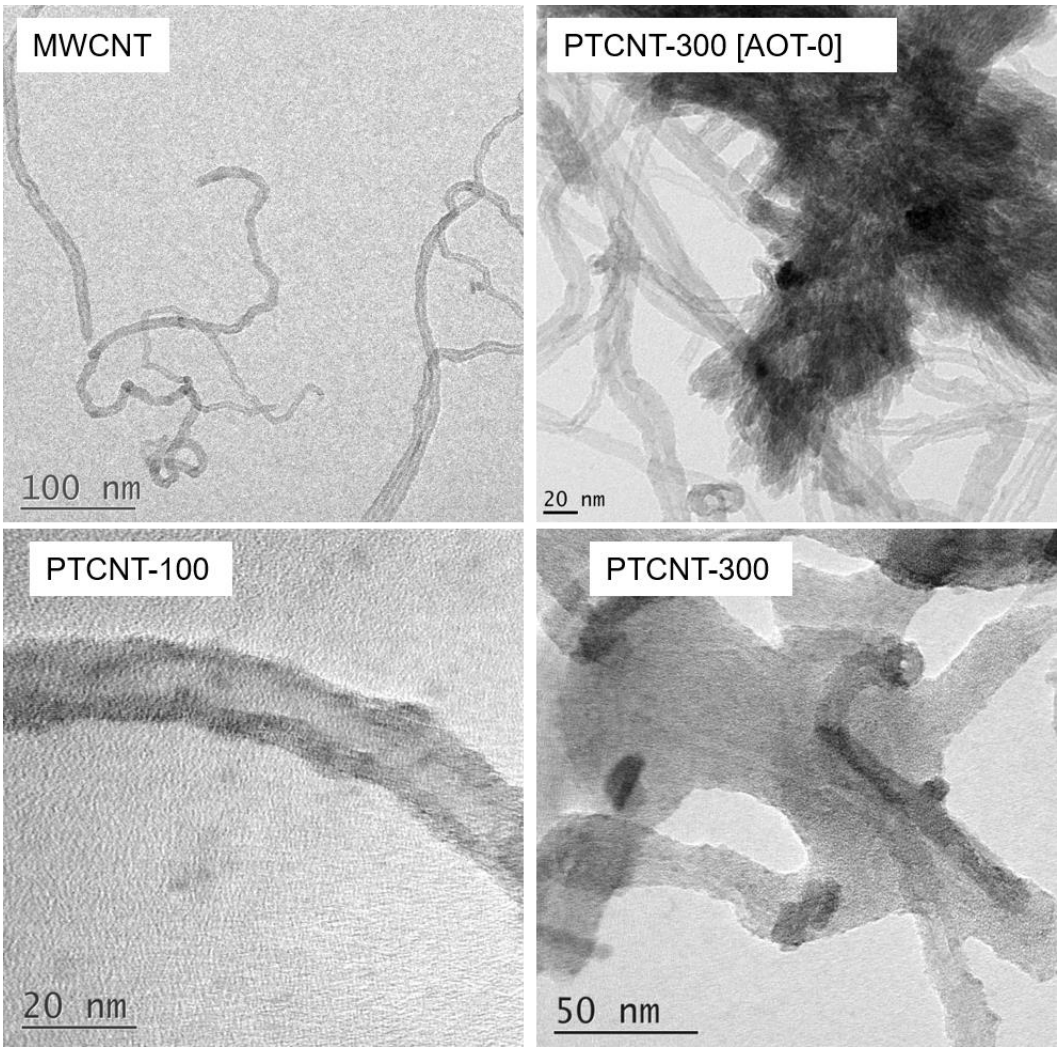

Figure 2.12. *Transmission electron microscopic (TEM) images of MWCNT, PTCNT-300 [AOT-0], PTCNT-100 and PTCNT-300*

The difference in the WXRD patterns of PTCNT-300 and PTCNT-300 [AOT-0] confirmed the notable role of surfactant AOT in the nanocomposite formation (see **Figure 2.13.**). The broad, amorphous peak of polythiophene was observed to be more suppressed in PTCNT-300 than in PTCNT-300 [AOT-0]. The graph was plotted for the intensity ratio of (002) plane of MWCNT (I_{CNT}) to amorphous polythiophene (I_{PT}) (see **Figure 2.13. inset**). The I_{CNT}/I_{PT} value was higher for PTCNT-300 than PTCNT-300[AOT-0] due to the suppression of the amorphous peak of polythiophene by pi-pi stacking interaction with MWCNT. Due to the inappropriate orientation of both components, the phase-separated polythiophene could not interact effectively with

MWCNT by weak non-covalent forces. The double-tailed AOT upholds the stacking interaction between polythiophene and MWCNT for the generation of core-shell PTCNT nanocomposites.

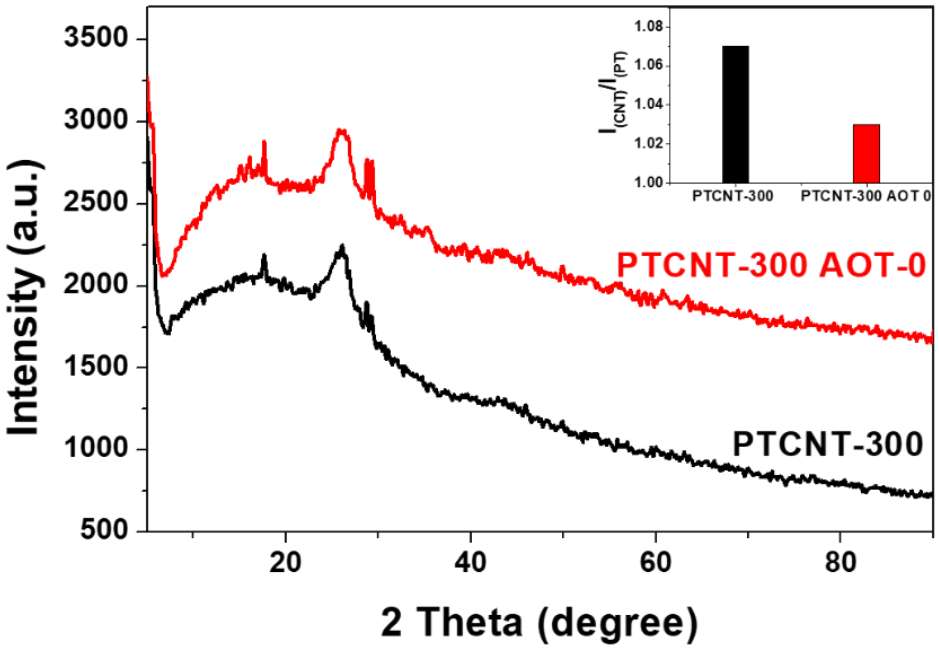

Figure 2.13. *WXRD patterns of PTCNT-300 and PTCNT-300[AOT-0]. Diagram exhibiting the ratio of I_{CNT} (intensity of characteristic peak of MWCNT) to I_{PT} (intensity of characteristic X-ray diffraction peak of polythiophene) for PTCNT-300 and PTCNT-300[AOT-0] (inset)*

2.3.5. Mechanism of composite formation

The formation mechanism of PTCNT nanocomposites was proposed based on the evidence obtained from FT-IR spectra, WXRD patterns and morphological analyses. Thiophene was polymerized in the presence of double tail surfactant sodium bis (2-ethyl hexyl) sulfosuccinate; the nearly spherical shaped polymer microparticles were formed. AOT and thiophene monomer in soluble form combined to form micellar aggregates complex in chloroform medium. Thiophene monomer gets oriented with the shape of micelles in chloroform, thereby stabilizing the monomer with spherical micelles. The addition of MWCNT to the AOT- thiophene micellar complex resulted in the migration of aggregates to the surface of MWCNT with the help of mild sonication. Entanglements of carbon nanotubes also get released up to a limit with the help of sonication-assisted micellar aggregate's interaction with the surface of nanotubes. Then the oxidative polymerization of thiophene with $FeCl_3$ causes the

polymer to grow up on the outer surface of MWCNT. As a result, a thick nano-layer instead of sub-microspheres formed in pure polymeric form. The mechanism of the PT and PTCNT composite formation is represented in **Figure 2.14.**

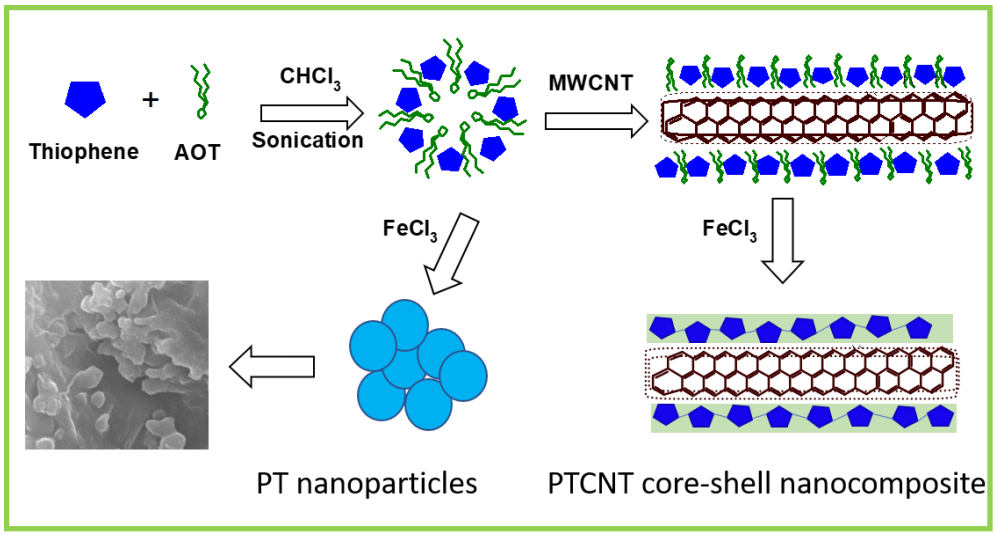

Figure 2.14. *Mechanism of the formation of PT-25 and PTCNT nanocomposites*

2.3.6. Enhancement of properties

The electrical conductivity of the samples was measured using Keithley four-probe electrical conductivity meter. The average conductivity measured at four points of the pelletized sample was taken as values. A graph was plotted for the average value of conductivity against the corresponding samples (see **Figure 2.15.**). Conductivity of PT-25[AOT-0], PT-25, PTCNT-100, PTCNT-200, PTCNT-300 and PTCNT-400 and MWCNT were 4.7×10^{-5}, 7.3×10^{-3}, 3.58×10^{-1}, 3.98×10^{-1}, 2.2×10^{-2}, 3.40×10^{-1} and 8.66 S/cm respectively.[40,41,65] PT-25 exhibited a higher value of conductivity relative to PT-25[AOT-0]. The enhancement in conductivity was due to the effective doping that occurred at the thiophene rings of PT-25. The AOT successfully enacted the role of dopant on the polymeric chains. The conductivity of PTCNT composites was observed as 1.5 times higher order of magnitude than PT-25. The conductivity enhancement in PTCNT nanocomposites was due to the effective charge transport between conducting polythiophene and multiwalled carbon nanotubes.

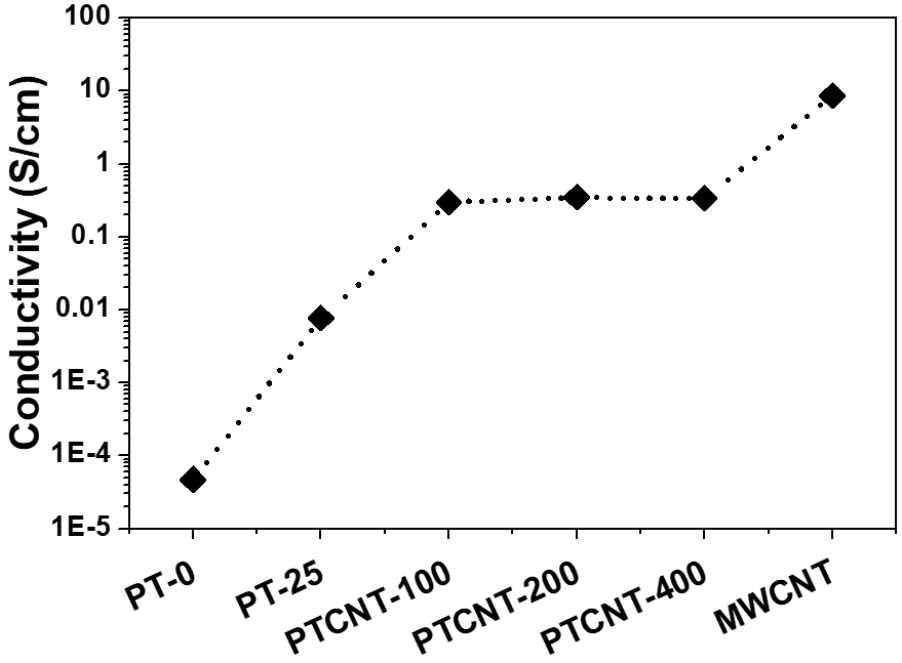

Figure 2.15. *Electrical conductivity of PT-0, PT-25, PTCNT-100, PTCNT-200, PTCNT-400 and pristine MWCNT.*

The inherent bundling nature of MWCNT made its dispersion uneasy. Mild sonication has power limits to separate the CNT bundles because of the lengthier CNT structure; however, strong sonication might shorten the CNT length and damage the CNT surface. MWCNT does not exhibit good dispersion in chloroform and water (see **Figure 2.16. A and B**). One of the effective ways to create the dispersible nature of carbon nanotubes was making MWCNT into nanocomposites with structurally similar polymers. Conducting polythiophene was utilized here to modify the surface of CNT to attain dispersible nature. Polythiophene-multiwalled carbon nanotube nanocomposites exhibited stable dispersion in chloroform with the assistance of mild sonication. Non-covalent forces working between polythiophene and MWCNT helped to overcome the self-aggregating nature of MWCNT. PTCNT nanocomposites have poor dispersion in an aqueous medium due to the polythiophene coating, which is hydrophobic in water (see **Figure 2.16. A and B**). The PTCNT-300[AOT-0], which was devoided AOT and poorly soluble in chloroform and water, exhibited a slight improvement in water dispersibility after adding AOT via sonicating for 15 minutes. Improvement could be attributed to the post-doping effect of AOT on polythiophene and its surfactant effect.

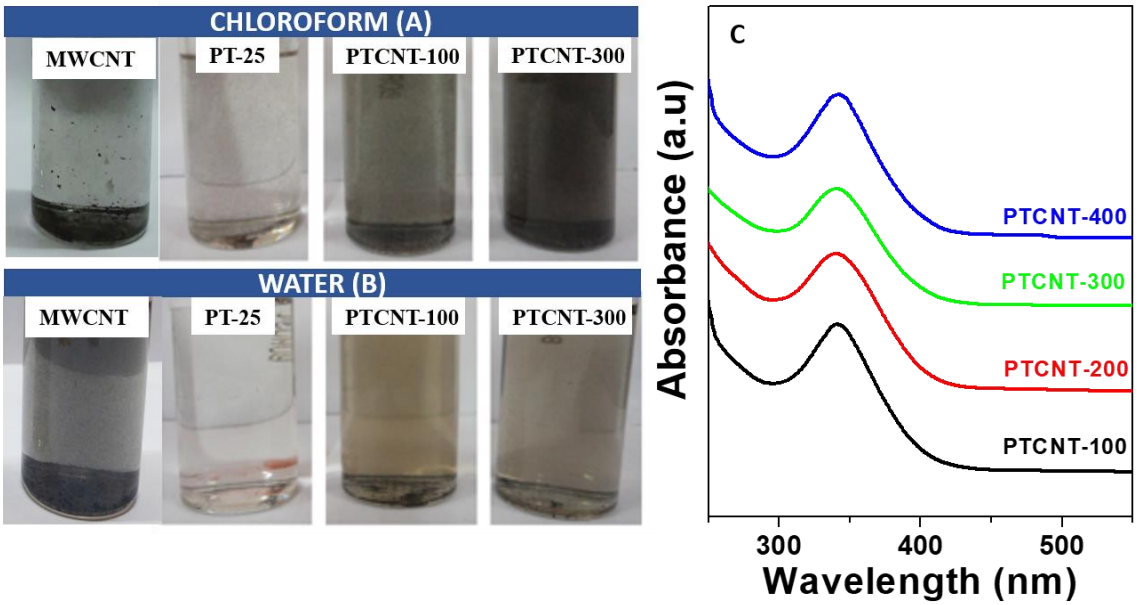

Figure 2.16. *Dispersions of MWCNT, PT-25, PTCNT-100 and PTCNT-300 in chloroform (A) and water (B). UV-vis absorption spectra of PTCNT-100, PTCNT-200, PTCNT-300 and PTCNT-400 recorded in chloroform medium (C).*

UV-vis absorption spectra of PTCNT-100, PTCNT-200, PTCNT-300 and PTCNT-400 in chloroform were shown in **Figure 2.16. C**. Stable dispersions of PTCNT composites in chloroform enabled to record UV-vis absorption spectra. A well-resolved characteristic peak corresponding to polythiophene was obtained at 340 nm due to the polaron-π transition in polythiophene chains.[46,66] UV-vis peak of PTCNT composites corresponding to carbon nanotubes (<275 nm) could not be resolved since it merged with the UV-solvent cut-off peaks of $CHCl_3$ solvent (240 and 260 nm).[67,68] Poor dispersibility of polythiophene and MWCNT carbon nanotubes hampered our efforts to take UV-vis absorption in chloroform. The dispersible nature of MWCNT was found to be improved by the addition of AOT surfactant.

Thermal stability of the samples PT-25, PTCNT-100 and PTCNT-300 were studied by thermogravimetric analysis (TGA). Thermograms of PT-25, PTCNT-100 and PTCNT-300 were recorded at a heating rate of 20°C/min in a nitrogen atmosphere (see **Figure 2.17.**). The polymer samples exhibited 10% weight loss when the temperature reached 250-280°C.[58,69] The composites PTCNT -100 and PTCNT-300 showed higher thermal stability than the polymer PT-25 in higher temperatures due to

incorporating a more thermally stable carbon nanotube. The weight percentage of polymer composite decreased to 65-75% in the temperature range of 500-600°C due to carbon decomposition from the polymer chain.

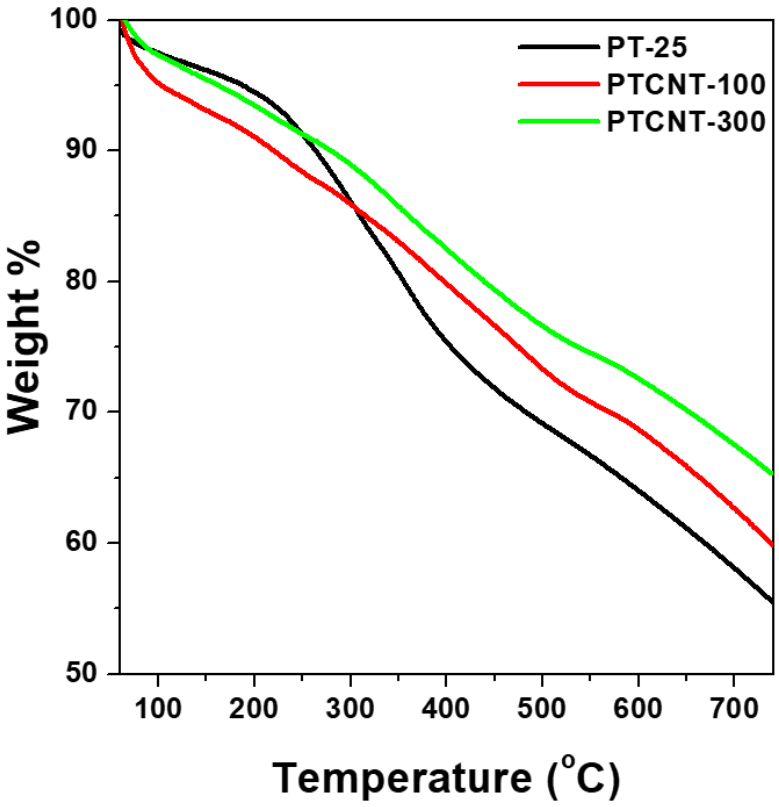

Figure 2.17. *Thermogravimetric analysis of PT-25, PTCNT-100 and PTCNT-300*

PTCNT binary composites have two major components; polythiophene (PT) and multiwalled carbon nanotubes (MWCNT). Thiophene was used as a monomer to obtain the polymeric component in the nanocomposite. Polythiophene thick coating prevents the self-aggregation of carbon nanotubes and produces dispersion in chloroform. The use of conducting polymer helped to maintain appreciably good conductivity value for composite by involving charge transport with carbon nanotube. Another component is MWCNT which was added as such to the reaction mixture. MWCNT was used as a permanent template for achieving morphologically distinctive nanofibrous structures. The major contribution of conductivity of nanocomposite came from carbon nanotubes' electronic structure. The presence of MWCNT is also the reason for the improved thermal stability of PTCNT nanocomposites. AOT was used in less proportion in the preparation stage to act as a surfactant supplement and dopant. The role of double tail surfactant sodium bis (2-ethyl hexyl) sulfosuccinate in nanocomposite formation and enhanced properties were notable based on different

analytical techniques such as X-ray diffraction, transmission electron microscopic imaging, UV-vis absorption spectra, monitoring dispersion stability and conductivity measurements. AOT acted as a stabilizing agent, dopant and surfactant in nanocomposite preparation stage. It also helps for stacking interaction between polymer and CNT; thereby responsible for the core-shell morphology of nanocomposite. Dispersion of nanocomposites were achieved with the help of stabilizing agent AOT. These stable dispersions enabled to record well-resolved peak in the UV-vis spectrum of nanocomposites (see **Figure 2.18.**).

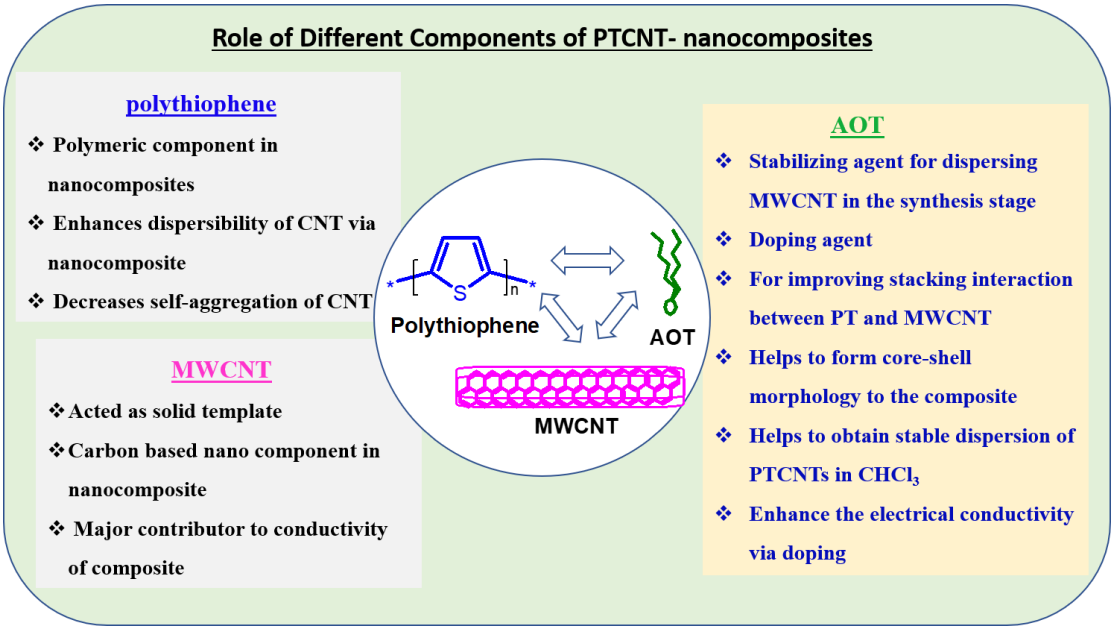

Figure 2.18. *Illustration of the role of polythiophene, MWCNT and AOT in the PTCNT nanocomposite formation.*

2.2. Conclusion

In conclusion, we have prepared polythiophene-multiwalled carbon nanotube nanocomposites (PTCNTs) via in-situ chemical oxidative polymerization of thiophene in the presence of AOT surfactant (monomer to surfactant mole ratio: 1:1/25). Polymerization was carried out using the oxidant $FeCl_3$ in chloroform medium. FT-IR spectroscopy characterizes the stretching and bending vibrations of polythiophene and MWCNT indicating the formation of the nanocomposite. The percentage of sulfur in elemental analysis validated the systematic increase of weight percentage of carbon nanotube in PTCNTs. X-ray diffraction pattern of nanocomposites exhibited a broad, amorphous peak of polythiophene with 2θ ranging from 12°-25° and a sharp peak from (002) plane of MWCNT centered at 26°. In WXRD scan, an increase in the intensity of

MWCNT diffraction peak and a decrease in the intensity of the amorphous peak of polythiophene was observed by adding a higher weight percentage of carbon nanotubes in the composites. Scanning electron micrographs of PTCNT-100 and PTCNT-300 displayed characteristic nanofibrous morphology. Transmission electron microscopic (TEM) images exhibited core-shell morphology to PTCNT-100 and PTCNT-300; CNT's tubular core was covered with a thick polythiophene shell. The outer shell diameter of nanocomposites was observed to be 3 to 12 nm increase than the outer tube diameter of pristine MWCNT. AOT has an inevitable role as a surfactant and dopant in forming core-shell morphology and π-π stacking interaction of PT with MWCNT in the nanocomposites. The well-resolved peak corresponding to the polaron-π transition in the polythiophene chain was obtained in the UV-vis spectrum of nanocomposites. Electrical conductivity enhancement in AOT-doped polythiophene (PT-25) and AOT-undoped polythiophene revealed the role of anionic surfactant AOT for stabilizing charges formed on conducting polymer chains on oxidation. The nanocomposite conductivity was 1.5 times higher-order in magnitude than PT-25 because effective charge transport occurred between conductive polythiophene and CNT. The nanocomposites also showed better thermal stability up to 500°C. In summary, results obtained from various analyses and enhanced properties of nanocomposites indicate the major role of AOT in the effective formation of solid state-ordered, conducting and dispersible core-shell PTCNT nanocomposites.

References

1. Gangopadhyay, R.; De, A. Conducting Polymer Nanocomposites: A Brief Overview. Chem. Mater. **2000**, 12 (3), 608–622. https://doi.org/10.1021/cm990537f.
2. Rajesh; Ahuja, T.; Kumar, D. Recent Progress in the Development of Nano-Structured Conducting Polymers/Nanocomposites for Sensor Applications. Sensors Actuators, B Chem. **2009**, 136 (1), 275–286. https://doi.org/10.1016/j.snb.2008.09.014.
3. Al-Mashat, L.; Shin, K.; Kalantar-Zadeh, K.; Plessis, J. D.; Han, S. H.; Kojima, R. W.; Kaner, R. B.; Li, D.; Gou, X.; Ippolito, S. J.; Wlodarski, W. Graphene/Polyaniline Nanocomposite for Hydrogen Sensing. J. Phys. Chem. C **2010**, 114 (39), 16168–16173. https://doi.org/10.1021/jp103134u.
4. Chang, C. M.; Weng, C. J.; Chien, C. M.; Chuang, T. L.; Lee, T. Y.; Yeh, J. M.; Wei, Y. Polyaniline/Carbon Nanotube Nanocomposite Electrodes with Biomimetic Hierarchical Structure for Supercapacitors. J. Mater. Chem. A **2013**, 1 (46), 14719–14728. https://doi.org/10.1039/c3ta13758a.
5. Liu, X.; Zheng, Y.; Wang, X. Controllable Preparation of Polyaniline-Graphene Nanocomposites Using Functionalized Graphene for Supercapacitor Electrodes. Chem. - A Eur. J. **2015**, 21 (29), 10408–10415. https://doi.org/10.1002/chem.201501245.

6. Tang, Q.; Cai, H.; Yuan, S.; Wang, X. Counter Electrodes from Double-Layered Polyaniline Nanostructures for Dye-Sensitized Solar Cell Applications. J. Mater. Chem. A **2013**, 1 (2), 317–323. https://doi.org/10.1039/c2ta00026a.
7. Dawan, F.; Jin, Y.; Goettert, J.; Ibekwe, S. High Functionality of a Polymer Nanocomposite Material for MEMS Applications. Microsyst. Technol. **2008**, 14 (9–11), 1451–1459. https://doi.org/10.1007/s00542-008-0577-4.
8. Ago, H.; Petritsch, K.; Shaffer, M. S. P.; Windle, A. H.; Friend, R. H. Composites of Carbon Nanotubes and Conjugated Polymers for Photovoltaic Devices. Adv. Mater. **1999**, 11 (15), 1281–1285. https://doi.org/10.1002/(SICI)1521-4095(199910)11:15<1281::AID-ADMA1281>3.0.CO;2-6.
9. Curran, S. A.; Ajayan, P. M.; Blau, W. J.; Carroll, D. L.; Coleman, J. N.; Dalton, A. B.; Davey, A. P.; Drury, A.; McCarthy, B.; Maier, S.; Strevens, A. A Composite from Poly(m-Phenylenevinylene-Co-2,5-Dioctoxy-p-Phenylenevinylene) and Carbon Nanotubes: A Novel Material for Molecular Optoelectronics. Adv. Mater. **1998**, 10 (14), 1091–1093. https://doi.org/10.1002/(sici)1521-4095(199810)10:14<1091::aid-adma1091>3.0.co;2-l.
10. Kim, J. Y.; Kim, M.; Kim, H. M.; Joo, J.; Choi, J. H. Electrical and Optical Studies of Organic Light Emitting Devices Using SWCNTs-Polymer Nanocomposites. Opt. Mater. (Amst). **2003**, 21 (1–3), 147–151. https://doi.org/10.1016/S0925-3467(02)00127-1.
11. Lu, X.; Zhang, W.; Wang, C.; Wen, T. C.; Wei, Y. One-Dimensional Conducting Polymer Nanocomposites: Synthesis, Properties and Applications. Prog. Polym. Sci. **2011**, 36 (5), 671–712. https://doi.org/10.1016/j.progpolymsci.2010.07.010.
12. Liu, Y.; Kumar, S. Polymer/Carbon Nanotube Nano Composite Fibers-A Review. ACS Appl. Mater. Interfaces **2014**, 6 (9), 6069–6087. https://doi.org/10.1021/am405136s.
13. Wang, L.; Lu, X.; Lei, S.; Song, Y. Graphene-Based Polyaniline Nanocomposites: Preparation, Properties and Applications. J. Mater. Chem. A **2014**, 2 (13), 4491–4509. https://doi.org/10.1039/c3ta13462h.
14. Kim, K. H.; Jo, W. H. A Strategy for Enhancement of Mechanical and Electrical Properties of Polycarbonate/Multi-Walled Carbon Nanotube Composites. Carbon N. Y. **2009**, 47 (4), 1126–1134. https://doi.org/10.1016/j.carbon.2008.12.043.
15. Karim, M. R.; Lee, C. J.; Lee, M. S. Synthesis and Characterization of Conducting Polythiophene/Carbon Nanotubes Composites. J. Polym. Sci. Part A Polym. Chem. **2006**, 44 (18), 5283–5290. https://doi.org/10.1002/pola.21640.
16. Mandal, A.; Nandi, A. K. Physical Properties of Poly(Vinylidene Fluoride) Composites with Polymer Functionalized Multiwalled Carbon Nanotubes Using Nitrene Chemistry. J. Mater. Chem. **2011**, 21 (39), 15752–15763. https://doi.org/10.1039/c1jm12926k.
17. Kałuża, D.; Jaworska, E.; Mazur, M.; Maksymiuk, K.; Michalska, A. Multiwalled Carbon Nanotubes-Poly(3-Octylthiophene-2,5-Diyl) Nanocomposite Transducer for Ion-Selective Electrodes: Raman Spectroscopy Insight into the Transducer/Membrane Interface. Anal. Chem. **2019**, 91 (14), 9010–9017. https://doi.org/10.1021/acs.analchem.9b01286.
18. He, P.; Shimano, S.; Salikolimi, K.; Isoshima, T.; Kakefuda, Y.; Mori, T.; Taguchi, Y.; Ito, Y.; Kawamoto, M. Noncovalent Modification of Single-Walled Carbon Nanotubes Using Thermally Cleavable Polythiophenes for Solution-Processed Thermoelectric Films. ACS Appl. Mater. Interfaces **2019**, 11 (4), 4211–4218. https://doi.org/10.1021/acsami.8b14820.
19. Gao, J.; Zhao, B.; Itkis, M. E.; Bekyarova, E.; Hu, H.; Kranak, V.; Yu, A.; Haddon, R. C. Chemical Engineering of the Single-Walled Carbon Nanotube-Nylon 6 Interface. J. Am. Chem. Soc. **2006**, 128 (23), 7492–7496. https://doi.org/10.1021/ja057484p.
20. Chen, J.; Ramasubramaniam, R.; Xue, C.; Liu, H. A Versatile, Molecular Engineering Approach to Simultaneously Enhanced, Multifunctional Carbon Nanotube-Polymer Composites. Adv. Funct. Mater. **2006**, 16 (1), 114–119. https://doi.org/10.1002/adfm.200500590.

21. Schmidt, G.; Malwitz, M. M. Properties of Polymer-Nanoparticle Composites. Curr. Opin. Colloid Interface Sci. **2003**, 8 (1), 103–108. https://doi.org/10.1016/S1359-0294(03)00008-6.
22. Heeger, A. J.; Sariciftci, N. S.; Namdas, B. E. Semiconducting and metallic polymers. 2010. ISBN: 9780198528647
23. Skotheim, T. A.; Reynlod, J. R. Handbook of Conducting Polymers, 2 Volume Set; 2007. https://doi.org/10.1201/b12346.
24. Dan, L. I.; Huang, J.; Kaner, R. B. Polyaniline Nanofibers: A Unique Polymer Nanostructure for Versatile Applications. Acc. Chem. Res. **2009**, 42 (1), 135–145. https://doi.org/10.1021/ar800080n.
25. Huang, J.; Virji, S.; Weiller, B. H.; Kaner, R. B. Nanostructured Polyaniline Sensors. Chem. - A Eur. J. **2004**, 10 (6), 1314–1319. https://doi.org/10.1002/chem.200305211.
26. Tyler McQuade, D.; Pullen, A. E.; Swager, T. M. Conjugated Polymer-Based Chemical Sensors. Chem. Rev. **2000**, 100 (7), 2537–2574. https://doi.org/10.1021/cr9801014.
27. Anderson, M. R.; Mattes, B. R.; Reiss, H.; Kaner, R. B. Conjugated Polymer Films for Gas Separations. Science (80-.). **1991**, 252 (5011), 1412–1415. https://doi.org/10.1126/science.252.5011.1412.
28. Dresselhaus, M. S.; Dresselhaus, G.; Avouris, P. Carbon nanotubes: Synthesis structure, properties, and applications. Springer, Heidelberg, **2001**, 80.
29. Ajayan, P. M. Nanotubes from Carbon. Chem. Rev. **1999**, 99 (7), 1787–1799. https://doi.org/10.1021/cr970102g.
30. Baughman, R. H.; Zakhidov, A. A.; De Heer, W. A. Carbon Nanotubes - The Route toward Applications. Science (80-.). **2002**, 297 (5582), 787–792. https://doi.org/10.1126/science.1060928.
31. Haddon, R. C. Carbon Nanotubes. Acc. Chem. Res. **2002**, 35 (12), 997. https://doi.org/10.1021/ar020259h.
32. Lee, T. Y.; Alegaonkar, P. S.; Yoo, J. B. Fabrication of Dye Sensitized Solar Cell Using TiO2 Coated Carbon Nanotubes. Thin Solid Films **2007**, 515 (12), 5131–5135. https://doi.org/10.1016/j.tsf.2006.10.056.
33. Conway, B. E. Electrochemical Supercapacitors; 1999. https://doi.org/10.1007/978-1-4757-3058-6.
34. Liu, Z.; Jiao, L.; Yao, Y.; Xian, X.; Zhang, J. Aligned, Ultralong Single-Walled Carbon Nanotubes: From Synthesis, Sorting, to Electronic Devices. Adv. Mater. **2010**, 22 (21), 2285–2310. https://doi.org/10.1002/adma.200904167.
35. Tuncel, D. Non-Covalent Interactions between Carbon Nanotubes and Conjugated Polymers. Nanoscale **2011**, 3 (9), 3545. https://doi.org/10.1039/c1nr10338e.
36. Tummala, N. R.; Morrow, B. H.; Resasco, D. E.; Striolo, A. Stabilization of Aqueous Carbon Nanotube Dispersions Using Surfactants: Insights from Molecular Dynamics Simulations. ACS Nano **2010**, 4 (12), 7193–7204. https://doi.org/10.1021/nn101929f.
37. Grossiord, N.; Loos, J.; Regev, O.; Koning, C. E. Toolbox for Dispersing Carbon Nanotubes into Polymers to Get Conductive Nanocomposites. Chem. Mater. **2006**, 18 (5), 1089–1099. https://doi.org/10.1021/cm051881h.
38. Zou, J.; Liu, L.; Chen, H.; Khondaker, S. I.; McCullough, R. D.; Huo, Q.; Zhai, L. Dispersion of Pristine Carbon Nanotubes Using Conjugated Block Copolymers. Adv. Mater. **2008**, 20 (11), 2055–2060. https://doi.org/10.1002/adma.200701995.
39. Zou, J.; Khondaker, S. I.; Huo, Q.; Zhai, L. A General Strategy to Disperse and Functionalize Carbon Nanotubes Using Conjugated Block Copolymers. Adv. Funct. Mater. **2009**, 19 (3), 479–483. https://doi.org/10.1002/adfm.200800542.
40. Dyke, C. A.; Tour, J. M. Overcoming the Insolubility of Carbon Nanotubes Through High Degrees of Sidewall Functionalization. Chem. - A Eur. J. **2004**, 10 (4), 812–817. https://doi.org/10.1002/chem.200305534.
41. Saini, V.; Li, Z.; Bourdo, S.; Dervishi, E.; Xu, Y.; Ma, X.; Kunets, V. P.; Salamo, G. J.; Viswanathan, T.; Biris, A. R.; Saini, D.; Biris, A. S. Electrical, Optical, and Morphological

Properties of P3ht-Mwnt Nanocomposites Prepared by In Situ Polymerization. J. Phys. Chem. C **2009**, 113 (19), 8023–8029. https://doi.org/10.1021/jp809479a.

42. Kuila, B. K.; Malik, S.; Batabyal, S. K.; Nandi, A. K. In-Situ Synthesis of Soluble Poly(3-Hexylthiophene)/Multiwalled Carbon Nanotube Composite: Morphology, Structure, and Conductivity. Macromolecules **2007**, 40 (2), 278–287. https://doi.org/10.1021/ma061548e.
43. Mishra, A. K.; Agrawal, N. R.; Das, I. Synthesis of Water Dispersible Dendritic Amino Acid Modified Polythiophenes as Highly Effective Adsorbent for Removal of Methylene Blue. J. Environ. Chem. Eng. **2017**, 5 (5), 4923–4936. https://doi.org/10.1016/j.jece.2017.09.017.
44. Jiang, C.; Chen, G.; Wang, X. High-Conversion Synthesis of Poly(3,4-Ethylenedioxythiophene) by Chemical Oxidative Polymerization. Synth. Met. **2012**, 162 (21–22), 1968–1971. https://doi.org/10.1016/j.synthmet.2012.09.008.
45. Lin, Y.; Zhou, B.; Fernando, K. A. S.; Liu, P.; Allard, L. F.; Sun, Y. P. Polymeric Carbon Nanocomposites from Carbon Nanotubes Functionalized with Matrix Polymer. Macromolecules **2003**, 36 (19), 7199–7204. https://doi.org/10.1021/ma0348876.
46. Mandal, A.; Nandi, A. K. Noncovalent Functionalization of Multiwalled Carbon Nanotube by a Polythiophene-Based Compatibilizer: Reinforcement and Conductivity Improvement in Poly(Vinylidene Fluoride) Films. J. Phys. Chem. C **2012**, 116 (16), 9360–9371. https://doi.org/10.1021/jp302027y.
47. Cho, K. Y.; Yeom, Y. S.; Seo, H. Y.; Park, Y. H.; Jang, H. N.; Baek, K. Y.; Yoon, H. G. Rational Design of Multiamphiphilic Polymer Compatibilizers: Versatile Solubility and Hybridization of Noncovalently Functionalized CNT Nanocomposites. ACS Appl. Mater. Interfaces **2015**, 7 (18), 9841–9850. https://doi.org/10.1021/acsami.5b01849.
48. Clavé, G.; Delport, G.; Roquelet, C.; Lauret, J. S.; Deleporte, E.; Vialla, F.; Langlois, B.; Parret, R.; Voisin, C.; Roussignol, P.; Jousselme, B.; Gloter, A.; Stephan, O.; Filoramo, A.; Derycke, V.; Campidelli, S. Functionalization of Carbon Nanotubes through Polymerization in Micelles: A Bridge between the Covalent and Non-covalent Methods. Chem. Mater. **2013**, 25 (13), 2700–2707. https://doi.org/10.1021/cm401312v.
49. Kang, Y.; Taton, T. A. Micelle-Encapsulated Carbon Nanotubes: A Route to Nanotube Composites. J. Am. Chem. Soc. **2003**, 125 (19), 5650–5651. https://doi.org/10.1021/ja034082d.
50. Tkalya, E. E.; Ghislandi, M.; de With, G.; Koning, C. E. The Use of Surfactants for Dispersing Carbon Nanotubes and Graphene to Make Conductive Nanocomposites. Curr. Opin. Colloid Interface Sci. **2012**, 17 (4), 225–232. https://doi.org/10.1016/j.cocis.2012.03.001.
51. Wang, Y.; Santos, P. J.; Kubiak, J. M.; Guo, X.; Lee, M. S.; Macfarlane, R. J. Multistimuli Responsive Nanocomposite Tectons for Pathway Dependent Self-Assembly and Acceleration of Covalent Bond Formation. J. Am. Chem. Soc. **2019**, 141 (33), 13234–13243. https://doi.org/10.1021/jacs.9b06695.
52. Wang, H. Dispersing Carbon Nanotubes Using Surfactants. Curr. Opin. Colloid Interface Sci. **2009**, 14 (5), 364–371. https://doi.org/10.1016/j.cocis.2009.06.004.
53. Gong, X.; Liu, J.; Baskaran, S.; Voise, R. D.; Young, J. S. Surfactant-Assisted Processing of Carbon Nanotube/Polymer Composites. Chem. Mater. **2000**, 12 (4), 1049–1052. https://doi.org/10.1021/cm9906396.
54. Czajka, A.; Hazell, G.; Eastoe, J. Surfactants at the Design Limit. Langmuir **2015**, 31 (30), 8205–8217. https://doi.org/10.1021/acs.langmuir.5b00336.
55. Giddings, L. D.; Olesik, S. V. A Study of AOT Reverse Micelles in Liquids at Ambient and High Pressure. Langmuir **1994**, 10 (9), 2877–2883. https://doi.org/10.1021/la00021a008.
56. Jang, J.; Yoon, H. Formation Mechanism of Conducting Polypyrrole Nanotubes in Reverse Micelle Systems. Langmuir **2005**, 21 (24), 11484–11489. https://doi.org/10.1021/la051447u.

57. Sheu, E. Y.; Chen, S. H.; Huang, J. S. Structure, Interaction, and Growth of Sodium Dodecyl-o-Xylenesulfonate Micelles in Aqueous Solutions. J. Phys. Chem. **1987**, 91 (6), 1535–1541. https://doi.org/10.1021/j100290a049.
58. Gök, A.; Omastová, M.; Yavuz, A. G. Synthesis and Characterization of Polythiophenes Prepared in the Presence of Surfactants. Synth. Met. **2007**, 157 (1), 23–29. https://doi.org/10.1016/j.synthmet.2006.11.012.
59. Liu, R.; Liu, Z. Polythiophene: Synthesis in Aqueous Medium and Controllable Morphology. Chinese Sci. Bull. **2009**, 54 (12), 2028–2032. https://doi.org/10.1007/s11434-009-0217-0.
60. Qiao, X.; Wang, X.; Mo, Z. The FeCl3-Doped Poly(3-Alkyithiophenes) in Solid State. Synth. Met. **2001**, 122 (2), 449–454. https://doi.org/10.1016/S0379-6779(00)00587-7.
61. Kiani, G.; Sheikhloie, H.; Rostami, A. Highly enhanced electrical conductivity and thermal stability of polythiophene/single-walled carbon nanotubes nanocomposite. Iran. Polym. J.2011, 20(8), 623-632.
62. Ballav, N.; Biswas, M. Preparation and Evaluation of a Nanocomposite of Polythiophene with Al2O3. Polym. Int. **2003**, 52 (1), 179–184. https://doi.org/10.1002/pi.1001.
63. Tian, Z. Q.; Jiang, S. P.; Liang, Y. M.; Shen, P. K. Synthesis and Characterization of Platinum Catalysts on Multiwalled Carbon Nanotubes by Intermittent Microwave Irradiation for Fuel Cell Applications. J. Phys. Chem. B **2006**, 110 (11), 5343–5350. https://doi.org/10.1021/jp056401o.
64. Xu, D.; Lu, P.; Dai, P.; Wang, H.; Ji, S. In Situ Synthesis of Multiwalled Carbon Nanotubes over LaNiO 3 as Support of Cobalt Nanoclusters Catalyst for Catalytic Applications. J. Phys. Chem. C **2012**, 116 (5), 3405–3413. https://doi.org/10.1021/jp211009g.
65. Lee, S. J.; Lee, J. M.; Cheong, I. W.; Lee, H.; Kim, J. H. A Facile Route of Polythiophene Nanoparticles via Fe3+-Catalyzed Oxidative Polymerization in Aqueous Medium. J. Polym. Sci. Part A Polym. Chem. **2008**, 46 (6), 2097–2107. https://doi.org/10.1002/pola.22544.
66. Philip, B.; Xie, J.; Chandrasekhar, A.; Abraham, J.; Varadan, V. K. A Novel Nanocomposite from Multiwalled Carbon Nanotubes Functionalized with a Conducting Polymer. Smart Mater. Struct. **2004**, 13 (2), 295–298. https://doi.org/10.1088/0964-1726/13/2/007.
67. Salami-Kalajahi, M.; Haddadi-Asl, V.; Behboodi-Sadabad, F.; Rahimi-Razin, S.; Roghani-Mamaqani, H. Properties of PMMA/Carbon Nanotubes Nanocomposites Prepared by "Grafting through" Method. Polym. Compos. **2012**, 33 (2), 215–224. https://doi.org/10.1002/pc.22141.
68. Grassi, G.; Scala, A.; Piperno, A.; Iannazzo, D.; Lanza, M.; Milone, C.; Pistone, A.; Galvagno, S. A Facile and Ecofriendly Functionalization of Multiwalled Carbon Nanotubes by an Old Mesoionic Compound. Chem. Commun. **2012**, 48 (54), 6836–6838. https://doi.org/10.1039/c2cc31884a.
69. Rohini Das, K.; Jinish Antony, M. Synthesis and Characterisation of Water Dispersible Copolymer Submicron Spheres of Poly-(Phenylenediamine-Co-N-Sulfopropyl Aniline) via Random Copolymerisation. Polymer (Guildf). **2016**, 87, 215–225. https://doi.org/10.1016/j.polymer.2016.01.078.